www.arpnjournals.com

# VAPOUR LIQUID EQUILIBRIUM DATA PREDICTION FOR BINARY SYSTEMS CONTAINING PROPANE

A. R. Moghadassi[1], M. R. Nikkholgh[1], S. M. Hosseini[1], F. Parvizian[1] and A. Sanaeirad[2]
[1]Department of Chemical Engineering, Faculty of Engineering, Arak University, Arak, Iran
[2]Department of Civil Engineering, Faculty of Engineering, Arak University, Arak, Iran
E-Mail: a_moghadassi@yahoo.com

**ABSTRACT**

In this research, the ability of multi-layer perceptron neural networks to estimate vapour liquid equilibrium (VLE) data have been studied. Four binary systems (R1270+R290, $CO_2$+R290, R125+R290, and R32+R290) have been investigated in the large ranges of temperature and pressure. These systems show different deviations from the Raoult's law. The networks with one hidden layer consist of five neurons are developed as the optimal structure. The networks were trained and then used as one-step tools without any iteration to estimate VLE data. For these binary systems, uncertainties in the ANNs results were not more than 0.126, 0.371, 0.221, and 0.613 %, respectively. In addition, the abilities of ANNs are shown by comparisons with Margules, Van Laar, and some other usual correlations. Results show capability of presented networks obviously.

**Keywords:** vapour liquid equilibrium, data prediction, propane, binary systems, ANN, Margules, Van Laar correlations.

## 1. INTRODUCTION

Modeling and control of equipments for different chemical processes require the vapour liquid equilibrium (VLE) data [1]. The VLE data are usually estimated using thermodynamic models based on the fundamental phase equilibrium criterion of equality of chemical potential in both phases [2]. This process is based on the gamma- phi calculation method. This method requires knowledge of the activity coefficients in the liquid ($\gamma$) and gas ($\phi$) phases for all the components. Several activity coefficient models such as NRTL, ASOG, UNIFAC, UNIQUAC, Wilson, and their modified forms have been devised to evaluate VLE [3-5]. Another method is based on equations of state (EoS). These methods are applied well to hydrocarbon systems. However, it is difficult to apply EoS for systems containing polar compounds [6]. These approaches because of their complexity are not suitable for the rapid prediction of vapour liquid equilibrium.

Artificial neural network (ANN) is an empirical tool, which is analogous to the behavior of biological neural structures. They have the ability to identify underlying highly complex relationships from input-output data. In fact, they define several empirical relations, each for a portion of the data [7]. Speed, simplicity, and capacity to learn are other advantages of ANNs compared to the classical methods. Therefore, they can be used very suitable to predict VLE data non-iteratively for any set of input parameters. Furthermore, this method does not require values of pure component or interaction properties. Recently ANNs have been used in the multifarious instances of thermodynamical problems. In the context of VLE data predictions using ANNs, can sign to the suggested networks to estimate compressibility factor for the vapour and liquid phases as a function of temperature and pressure for several refrigerants [8], prediction of activity coefficient of liquid phase [9], calculation of VLE data for a light hydrocarbon mixture [10], benzene + hexane system [11], methane + ethane and ammonia +

water systems and systems containing polar compounds [6], carbon dioxide + difluoromethane system [12], tert-butanol + 2-ethyl-1-hexanol and n-butanol + 2-ethyl-1-hexanol systems [13], apply three multi-layer networks to calculate logarithm of activity coefficient ($\gamma$) based on sign (positive or negative) of ln $\gamma$ [14], and estimation of VLE data for binary and ternary systems using Radial Base Function (RBF) neural networks [7], etc.

In this research, multi-layer perceptron networks have been used to estimate vapour-liquid equilibrium data. Multi-layer networks are quite powerful. For instance, a network containing two layers, where the first and the second layer have sigmoid and linear functions respectively, can be trained to approximate any function (with a finite number of discontinuities) arbitrarily well [15].

Four typical binary refrigerant systems containing propane (R290) have been investigated in the large ranges of temperature and pressure. According to Raoult's law for an ideal mixture, the mole fractions of a component in the vapour and liquid phases are proportional [16]. A real mixture behaves differently. Therefore, the presented systems are categorized into four groups, based on their deviations from ideality: small positive deviation (R1270+R290), big positive deviation ($CO_2$+R290), and strong positive deviation with the presence of an azeotrope and minimum boiling point (R125+R290), and very strong positive deviation with the presence of an azeotrope and minimum boiling point (R32+R290). We have not found any previous literatures to apply ANNs to estimate vapour liquid equilibrium data in these systems.

The developed network for each mentioned system is trained and evaluated by using several sets of collected experimental data from literatures [17-21]. A portion of the experimental data was used to train the network and the rest was used to evaluate the performance of the networks. Experimental data and predicted values by ANNs are compared. Then, results are shown

graphically and deviations are presented. In addition, VLE data sets are correlated by using Margules and van Laar correlations. Then, the abilities of ANNs are shown by comparisons with Margules, van Laar, and some other usual correlations.

## 2. ARTIFICIAL NEURAL NETWORKS

An ANN can be considered as a black box consisting of a series of complicated equations for the calculation of outputs based on a given series of input values. One of the major advantages of ANN is efficient handling of highly nonlinear relations in data, even when the exact nature of such relation is unknown [22]. Commonly neural networks are trained; so that a particular input leads to a specific target output. The network is adjusted based on a comparison between the network outputs and the targets (real values of outputs), until the network outputs match the target [15].

The most popular ANN is the feed-forward multi-layer ANN which uses back-propagation learning algorithm. Feed-forward neural network usually has one or more hidden layers and an output layer. Scaled data is introduced into the input layer of the network and then is propagated from input layer to hidden layers and finally to the output layer.

Each layer consists of some cells, known as neurons. A parameter $W_{ij}$ (known as weight) is associated with each connection between two cells. Each neuron in hidden or output layer firstly acts as a summing junction, which combines and modifies the inputs from the previous layer using the following equation [22]:

$$A_j = b_j + \sum_{j=1}^{n} X_j W_{ij} \qquad (1)$$

$$Y_j = S(A_j) \qquad (2)$$

Where $X_j$ are the inputs to $j$th neuron (outputs from previous layer), $W_{ij}$ are the weights representing the strength of the connection between the $i$th neuron in the previous layer and $j$th neuron, $b_j$ is the bias associated with $j$th neuron, and $A_j$ is the net input of $j$th neuron in hidden or output layer. Each neuron consists of a transfer function. Output of a neuron is determined by transforming its net input using a suitable transfer function, namely $S$ in this work. Generally, the transfer functions for function approximation are sigmoidal function, hyperbolic tangent and linear function, that sigmoidal function is widely used for nonlinear relationship. $Y_j$ (The output of $j$th neuron) is also an element of inputs to neurons in the next layer [22].

There are many variations of the back-propagation algorithm. The simplest implementation of back-propagation learning, updates the network weights and biases in the direction in which the performance function decreases most rapidly - the negative of error gradient. An iteration of this algorithm can be written as:

$$V_{k+1} = V_k - \alpha_k g_k \qquad (3)$$

Where $V_k$ is a vector of current weights and biases, $g_k$ is the current gradient, $\alpha_k$ is the learning rate, and $V_{k+1}$ is a vector of new weights and biases. The objective is to find the values of the weights and biases that they minimize differences between the targets and the predicted outputs in order to minimize the mean square errors (MSE). MSE is the average squared error between the network predicted outputs and the target outputs.

The Levenberg-Marquardt algorithm is one of the best training rules designed to approach second-order network training speed [15]. This algorithm trains a neural network 10 to 100 faster than the usual gradient descent back-propagation method and uses the following update rule:

$$V_{k+1} = V_k - [J^T J + \mu \ I]^{-1} J^T e \qquad (4)$$

Where $J$ is the Jacobian matrix contained first derivatives of the network errors with respect to the weights and biases, $e$ is a vector of network errors, and $I$ is always a ones square matrix that is the same size as the $J^T J$. The Jacobian matrix can be computed through a standard back-propagation technique. The scalar $\mu$ decreases after each successful step (reduction in performance function) and increases only when a tentative step would increase the performance function. In this way, the performance function will reduce at any iteration of algorithm [15].

In the learning process, there are several variables that have influence on the ANN training. These variables are the number of iterations, learning rate, the momentum coefficient, number of hidden layers and the number of hidden neuron. To find the best set of these variables and parameters, all of those must be varied and the best combination should be chosen [15].

## 3. DEVELOPMENT OF ANN MODELS

After determining the number of input variables by using statistical analyses, the most appropriate architecture for the network should be determined. In this stage, several networks should be created, trained and tested. The number of layers, the optimum number of neurons per layers and the transfer function(s) in the hidden layer (s), obtain by trial and error. Care was taken to avoid overtraining. As a rule of thumb, the number of adjustable parameters should be equal or smaller than the number of available training data [22]. Numbers of adjustable parameters are related to neuron numbers directly. Therefore, several feed-forward neural networks with different architectures were tried. Finally, a feed-forward multi-layer perceptron network with one hidden layers is used which temperature, pressure, and mole fraction of the first compound in the liquid phase ($T$, $P$, $x_1$) are input variables and mole fraction of the first compound in the vapour phase ($y_1$) is output variable. A simple scheme of developed networks is shown in Figure-1. It has been proven that utilizing hyperbolic tangent sigmoid and

www.arpnjournals.com

linear transfer functions in the hidden and outer layers respectively will produce better results.
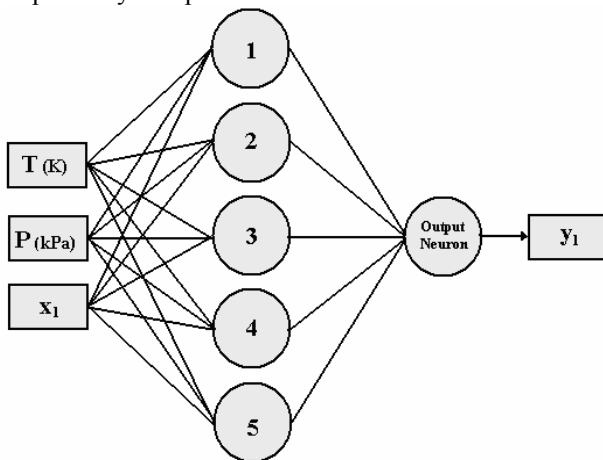


**Figure-1.** The schematic of Multi-layer perceptron with one hidden layer.

The input and output data are normalized in the range of [-1, 1], before import to networks. Then the Levenberg-Marquardt back-propagation algorithm that represents a simplified version of Newton's method is applied as the training algorithm in this study. This algorithm appears to be the fastest method for training moderate-sized feed-forward neural networks up to several hundred weights [15]. The mean squared error (MSE) as an excellent criterion for evaluating the performance of the neural network is used. Furthermore, the network was trained in MATLAB 7.0 environment.

## 4. RESULTS AND DISCUSSIONS

The optimum performance for the networks obtained iteratively by changing the number of neurons in the hidden layers. If there are a few neurons in the hidden layer, the performance of the network is not satisfactory. However, if there are too many, convergence is very slow and may be compromised by local minima. The optimal number of hidden neurons is determined empirically, as the minimal number of neurons for which the prediction performance is sufficient without leading to over fitting or an unreasonably long computational time. Finally, a model containing 5 hidden neurons are selected. The training and evaluating errors for binary systems are reported in Table-1.

**Table-1.** Deviation of training and testing stages for binary systems.

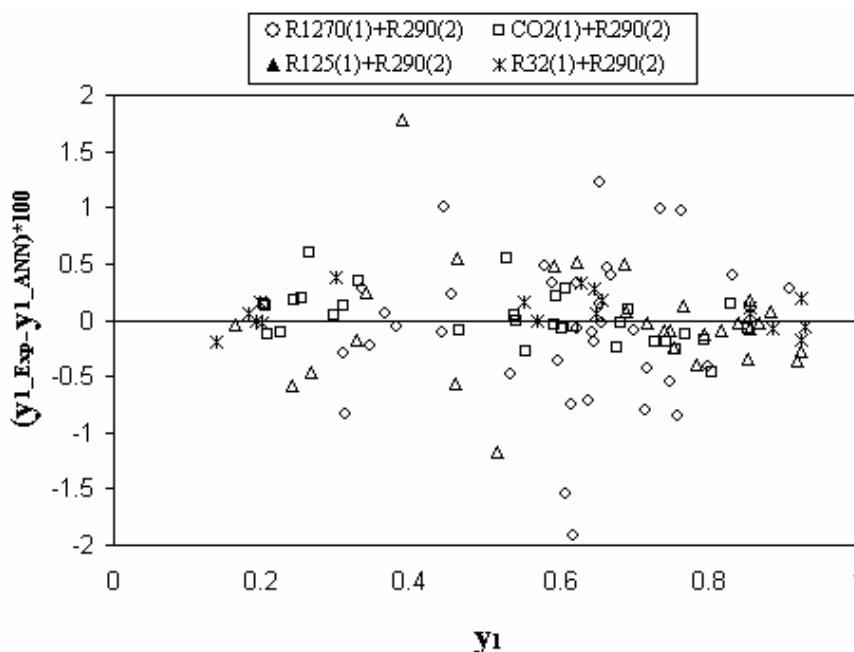| Binary mixture | Train | | Test | |
|---|---|---|---|---|
| | MSE | AAD % | MSE | AAD % |
| R125+R290 | 4.19e-6 | 0.159 | 5.3e-6 | 0.181 |
| $CO_2$+R290 | 1.27e-5 | 0.280 | 2.49e-5 | 0.334 |
| R32+R290 | 2.83e-5 | 0.418 | 4.47e-5 | 0.511 |
| RE1270+R290 | 9.84e-7 | 0.079 | 3.02e-6 | 0.139 |
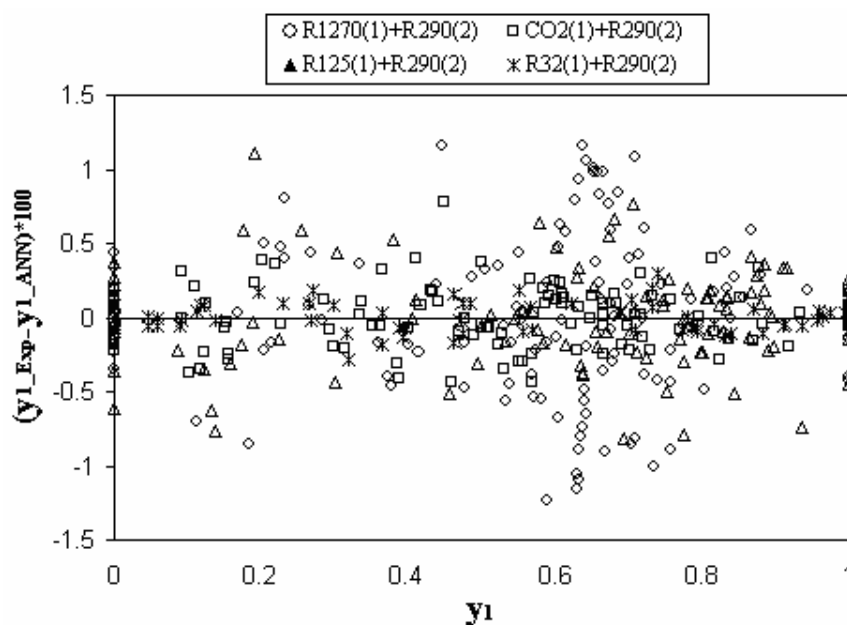


**Figure-2.** Percent deviation of ANN results against the used experimental data in the training process.

# ARPN Journal of Engineering and Applied Sciences

www.arpnjournals.com

The average absolute deviation is defined as below. The absolute deviation is defined as to avoid dividing by zero in the relative error $((y_1^{calc.} - y_1^{exp.})/y_1^{exp.})$, when mole fraction of the first compound in the vapour phase is zero.

$$AAD(\%) = \sum_{i=1}^{n} (y_1^{calc.} - y_1^{exp.})_i *100/n \qquad (5)$$



**Figure-3.** Percent deviation of ANN results against the used experimental data in the testing process.

As it is cleared, the values of absolute deviation in the training and testing stages for all binary systems are below than 1.5 % and 2 %, respectively.

Vapour-liquid composition (*x-y*) was calculated using developed networks. The estimated results of vapour–liquid composition in one temperature for each system are shown in Figure-4, summarily.

An extended report of results is presented in Table-2. In this table, temperatures, pressure ranges, in addition, average absolute deviation (*AAD %*) of unseen data for predicted vapour phase mole fraction data ($y_I$) in each temperature are presented for all binary systems.

As it is specified, for binary system of R32+R290 maximum deviation in predicted data is related to temperature of 283.15 K and pressure range of 0.280 to 0.689, equal 0.613 %. This is an excellent result for prediction of VLE data in a wide range of temperatures and pressures. For other mixtures, results are more accurate than this. As for binary systems of R1270+R290, $CO_2$+R290, and R125+R290 maximum values of the deviation (AAD %) were not more than 0.126, 0.371, and 0.221, respectively. These results show capability of presented network, obviously.

In addition, some models of the excess Gibbs energy and subsequent activity coefficients for binary

The admirable agreement between experimental data and predicted results by using neural models are shown, obviously. The accuracy of results in the training and testing stages are shown in Figures 2 and 3.

systems are used to correlate VLE data. Then their results are used as a criterion to evaluate the ANNs abilities. The three-suffix Margules and van Laar equations [23] are selected because they are mathematically easier to handle than the newer ones (Wilson, NRTL, and UNIQUAC). These equations include two empirical constants, to represent activity coefficient data. The equations are rearranged in a linear form to evaluate their constants.

Three-suffix Margules:

$$G^E = x_1 x_2 [A + B(x_1 - x_2)]$$

(6)

$$RT \ln \gamma_1 = (A + 3B)x_2^2 - 4Bx_2^3 \qquad (7)$$

$$RT \ln \gamma_2 = (A - 3B)x_1^2 + 4Bx_1^3 \qquad (8)$$

**Linear form:**

$$G^E / x_1 x_2 = (A - B) + 2Bx_1 \qquad (9)$$

**Van Laar:**

$$G^E = Ax_1 x_2 /[x_1(A/B) + x_2] \qquad (10)$$

$$RT \ln \gamma_1 = A(1 + Ax_1/(Bx_2))^{-2} \qquad (11)$$

$$RT \ln \gamma_2 = B(1 + Bx_2/(Ax_1))^{-2} \qquad (12)$$

www.arpnjournals.com

**Linear form:**

$$x_1 x_2 / G^E = 1/A + (1/B - 1/A)x_1 \qquad (13)$$

Where GE is the excess Gibbs energy; yi is activity coefficient of component i; xi is liquid phase mole fraction of component i; A, and B are the adjustable parameters of correlations. The excess Gibbs energy data are produced from TPxy experimental data of binaries by using equations 14 and 15. It is supposed that the liquid phase properties are independent of the pressure variations [3].

$$\gamma_i = y_i \hat{\phi}_i P /(x_i \phi_i^{sat} P_i^{sat}) \qquad i = 1,2$$
(14)

$$G^E = RT \sum_{i=1}^{2} x_i \ln \gamma_i$$
(15)

Where P, R, T, yi, Pisat, $\hat{\phi}_i$, and $\phi_i^{sat}$ are pressure, the gases constant, temperature, the vapor phase mole fraction of component i,  vapor pressure of component i, fugacity coefficient of component i in the vapor phase, fugacity coefficient of pure i at T and saturation pressure, respectively. The vapor pressure data of pure components is given in Table-3.
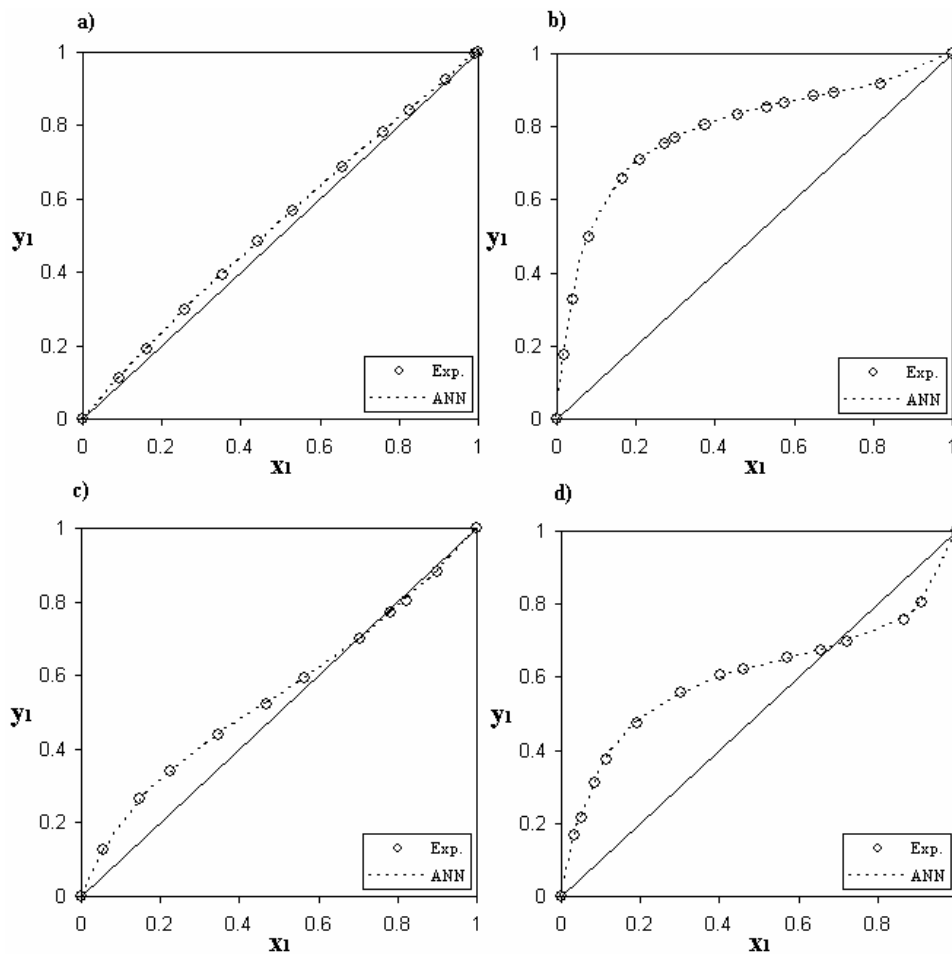


**Figure-4.** Vapour-liquid composition, a) binary system of R1270+R290 at 273.15 K, b) binary system of $CO_2$+R290 at 263.15, c) binary system of R125+R290 at 323.15 K, d) binary system of R32+R290 at 283.15 K.

www.arpnjournals.com

**Table-2.** Deviations of data sets for binary systems at different temperatures [23].

| Binary | Temp., K | Press. range, kPa | AAD % | Temp., K | Press. range, MPa | AAD % |
|---|---|---|---|---|---|---|
| R1270+ R290 | | | | | | |
| | 273.15 | 474.0-586.0 | 0.063 | 293.15 | 836.2-1019.0 | 0.126 |
| | 278.15 | 550.8-678.5 | 0.059 | 303.15 | 1077.6-1307.6 | 0.088 |
| | 283.15 | 636.0-780.8 | 0.088 | 313.15 | 1368.0-1652.2 | 0.116 |
| CO$_2$+R290 | | | | | | |
| | 253.15 | 309.2-1964.8 | 0.438 | 293.15 | 836.3-5723.7 | 0.346 |
| | 263.15 | 423.1-2641.8 | 0.198 | 303.15 | 1079.6-7206.2 | 0.221 |
| | 273.15 | 473.9-3113.2 | 0.220 | 313.15 | 1369.8-6434.3 | 0.311 |
| | 283.15 | 636.3-4497.8 | 0.259 | 323.15 | 1714.5-6281.3 | 0.371 |
| R125+R290 | | | | | | |
| | 253.15 | 244.1-426.7 | 0.221 | 288.15 | 731.0-1153.2 | 0.098 |
| | 258.15 | 292.2-461.9 | 0.182 | 293.15 | 836.9-1383.5 | 0.149 |
| | 263.15 | 345.5-586.4 | 0.207 | 303.15 | 1077.4-1798.5 | 0.200 |
| | 273.15 | 474.2-815.3 | 0.072 | 313.15 | 1373.2-2246.6 | 0.158 |
| | 283.15 | 635.6-1060.6 | 0.188 | 323.15 | 1716.2-2807.6 | 0.158 |
| R32+R290 | | | | | | |
| | 248.13 | 203.4-466.1 | 0.613 | 293.15 | 836.9-1824.1 | 0.282 |
| | 253.15 | 244.1-557.4 | 0.594 | 294.91 | 874.8-1902.3 | 0.503 |
| | 254.15 | 253.3-575.2 | 0.570 | 303.15 | 1078.3-2328.7 | 0.276 |
| | 263.15 | 345.5-777.6 | 0.476 | 313.15 | 1373.2-2946.6 | 0.219 |
| | 273.15 | 473.9-1054.8 | 0.494 | 323.15 | 1716.2-3674.1 | 0.422 |
| | 283.15 | 635.6-1402.1 | 0.282 | | | |

**Table-3.** Vapour pressure of pure compounds.

| R290 | | R1270 | | CO$_2$ | | R125 | | R32 | |
|---|---|---|---|---|---|---|---|---|---|
| T, K | P, kPa | T, K | P, kPa | T, K | P, kPa | T, K | P, kPa | T, K | P, kPa |
| 253.15 | 244.1 | 273.15 | 586.0 | 253.15 | 1964.8 | 253.15 | 338.5 | 253.15 | 406.2 |
| 263.15 | 345.5 | 278.15 | 678.5 | 263.15 | 2641.8 | 263.15 | 483.3 | 263.15 | 582.9 |
| 273.15 | 473.9 | 283.15 | 780.8 | 273.15 | 3478.5 | 273.15 | 670.9 | 273.15 | 813.8 |
| 283.15 | 635.6 | 293.15 | 1019.0 | 283.15 | 4497.8 | 283.15 | 909.5 | 283.15 | 1109.3 |
| 293.15 | 836.9 | 303.15 | 1307.6 | 293.15 | 5723.7 | 293.15 | 1206.7 | 293.15 | 1478.2 |
| 303.15 | 1078.3 | 313.15 | 1652.2 | 303.15 | 7206.2 | 303.15 | 1569.2 | 303.15 | 1930.2 |
| 313.15 | 1373.2 | | | | | 313.15 | 2009.3 | 313.15 | 2481.0 |
| 323.15 | 1716.2 | | | | | 323.15 | 2535.8 | 323.15 | 3144.7 |

The fugacity coefficients are calculated by using the virial equation in the vapor phase [16]. For binary systems activity coefficient calculate as below:

$$\ln \gamma_i = \ln \frac{y_i P}{x_i P_i^{sat}} + \frac{B_{ii}(P - P_i^{sat}) + P\delta_{12}(1 - y_i)^2}{RT} \quad i = 1, 2 \tag{16}$$

$$\delta 12 = 2B_{12} - B_{11} - B_{22} \tag{17}$$

Where $B_{ii}$ are the second virial coefficients. These coefficients are calculated by using the Pitzer equations extended for mixture by Prausnitz [3].
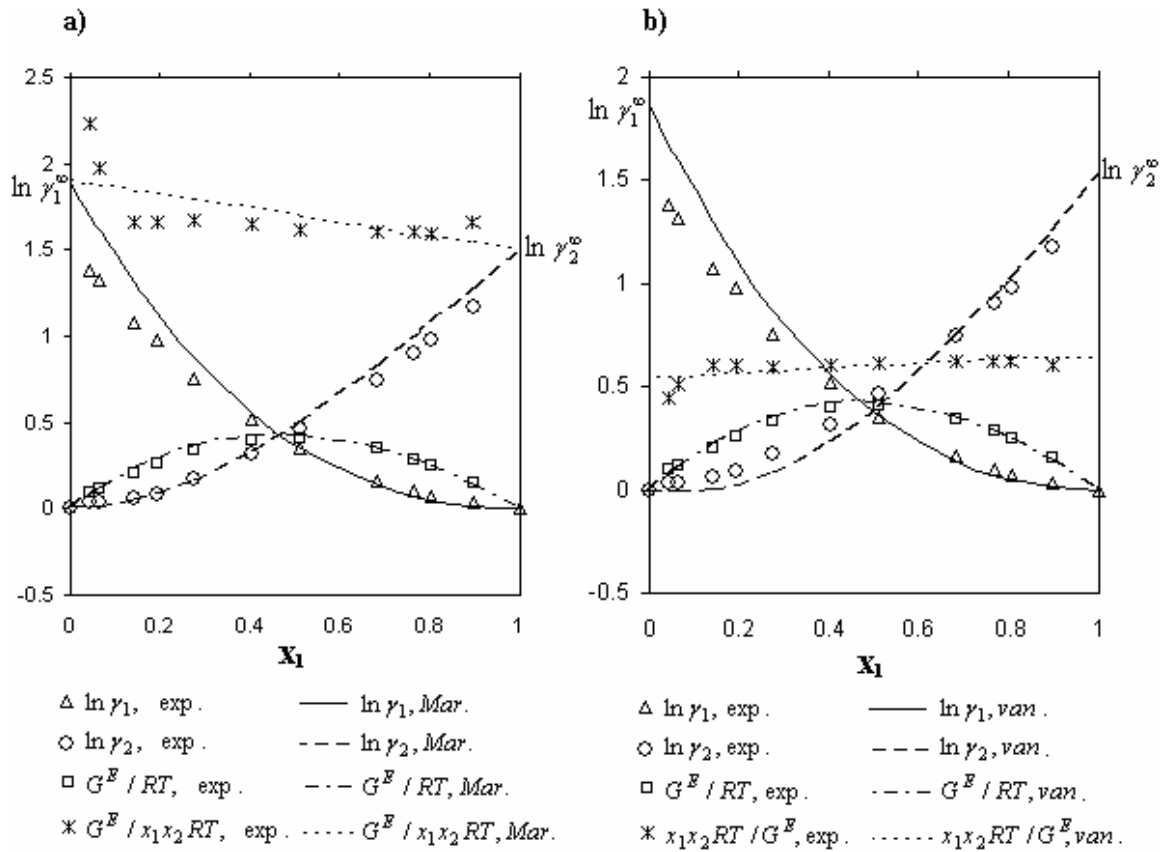
www.arpnjournals.com

Samples of the correlations for binary system of R125+R290 at 253.15 K are shown in Figure-5. In addition, for all binary systems in the whole of temperature ranges, deviations between correlation results and experimental data for vapour phase mole fraction of first compounds are shown in Figures 6 and 7. The deviations are about 3 and 4 %, respectively for Margules and van Laar correlations. As it is clear, these results are in the lower accuracy than the ANNs estimations.

The quantitative comparisons of these models as well as some other models used in the literatures for these systems are presented in Table-4. Results show the ability of ANNs in contrast with other models. However, some models have better results than ANNs, for example RKS EoS with the Huron-Vidal mixing rule and NRTL model [21], PR and CSD EoSs using the Wong-Sandler mixing rule [24] for binary system of R32 + R290; but the complexities of these models cause that the ANNs will be recommended as a successful tool to estimate VLE data.

**Table-4.** Comparison among results of different methods in the estimation of the first compounds vapour phase mole fraction.

| Binary | Model | Ref. | Temp. range (K) | AAD (%) |
|---|---|---|---|---|
| R1270+ R290: | | | | |
| | ANN | this work | 273.15-313.15 | $0.091^a$ |
| | Margules | this work | 273.15-313.15 | $0.335^a$ |
| | van Laar | this work | 273.15-313.15 | $0.317^a$ |
| | PR-EoS combined with the Wong-Sandler mixing rule | [17] | 273.15-313.15 | $0.254^a$ |
| | Van Laar | [25] | 261.11-361.11 | $0.150^b$ |
| | perturbed hard sphere EoS | [26] | 230.00-350.00 | $2.000^b$ |
| CO2+ R290: | | | | |
| | ANN | this work | 253.15-323.15 | $0.293^a$ |
| | Margules | this work | 253.15-303.15 | $7.554^a$ |
| | van Laar | this work | 253.15-303.15 | $7.471^a$ |
| | PR EoS with the van der Waals one fluid mixing rule | [19] | 253.15-323.15 | $0.660^b$ |
| | PR EoS with one constant binary interaction parameter | [19] | 253.15-323.15 | $0.750^b$ |
| | Redlich-Kwong EoS with a modified procedure | [27] | 224.44-266.66 | $0.657^a$ |
| R125+ R290: | | | | |
| | ANN | this work | 253.15-323.15 | $0.164^a$ |
| | Margules | this work | 253.15-323.15 | $3.629^a$ |
| | van Laar | this work | 253.15-323.15 | $3.719^a$ |
| | PR EoS using one parameter van der Waals one fluid model | [20] | 253.15-323.15 | $0.630^b$ |
| | RKS EoS | [18] | 258.15-303.15 | $0.312^a$ |
| R32+ R290: | | | | |
| | ANN | this work | 248.13-323.15 | $0.439^a$ |
| | Margules | this work | 248.13-323.15 | $6.064^a$ |
| | van Laar | this work | 248.13-323.15 | $5.915^a$ |
| | PR EoS using one parameter van der Waals one fluid model | [21] | 253.15-323.15 | $0.620^b$ |
| | RKS EoS with the Huron-Vidal mixing rule and NRTL model | [21] | 248.13-293.15 | $0.376^a$ |
| | PR EoS using the Wong-Sandler mixing rule | [24] | 268.15-313.15 | $0.340^a$ |
| | CSD EoS using the Wong-Sandler mixing rule | [24] | 268.15-313.15 | $0.370^a$ |
| | PR EoS using the Wong-Sandler mixing rule | [28] | 268.15- 318.15 | $1.026^a$ |
| | Carnahan-Starling-Desantis EoS | [28] | 268.15- 318.15 | $0.853^a$ |

$$^a\, AAD\% = 100/n * \sum_{i=1}^{n} \left|(y_{\exp} - y_{cal})\right|, \qquad ^b\, AAD\% = 100/n * \sum_{i=1}^{n} \left|(y_{\exp} - y_{cal})/y_{cal.}\right|$$
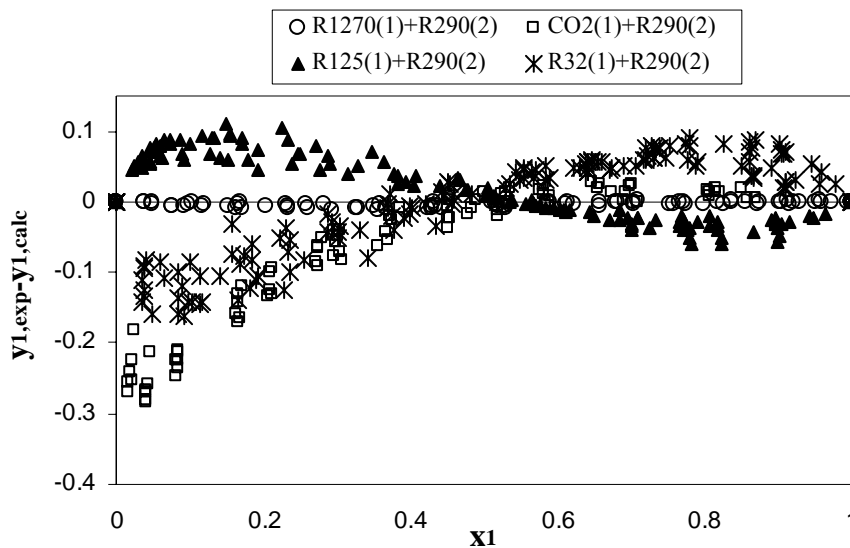
www.arpnjournals.com



**Figure-5.** The correlations of liquid phase properties for binary system of R125+R290 at 253.15 K using a) Margules and b) van Laar equations.
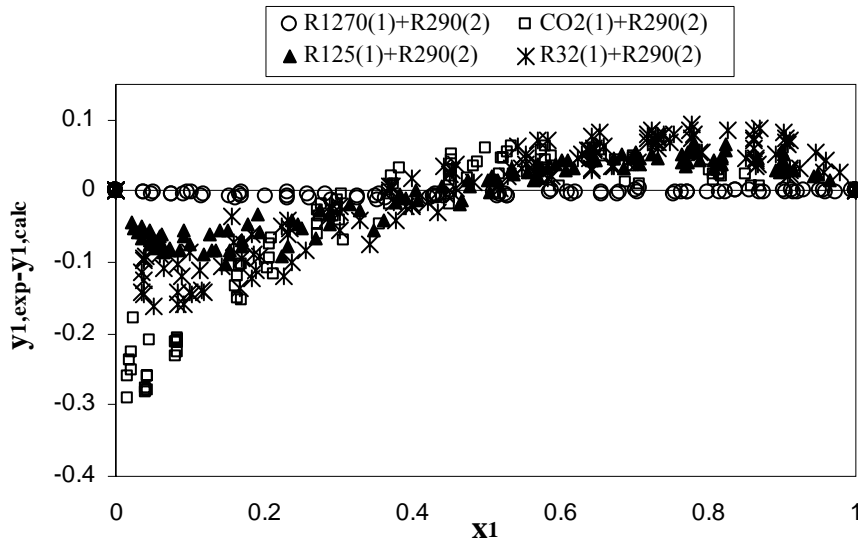


**Figure-6.** Deviations between Margules equation results and experimental data for binary systems in the whole of temperature ranges.

www.arpnjournals.com



**Figure-7.** Deviations between Van Laar equation results and experimental data for all binary systems in the whole of temperature ranges.

## 5. CONCLUSIONS

The ability of Artificial Neural Networks based on back-propagation algorithm to predict vapour liquid equilibria data of binary systems have been investigated. Therefore, four typical binary refrigerant systems with different non-ideally behavior, consist of propane (R290) have been studied in the large range of temperature and pressure.

Multi-layer perceptron networks with one hidden layer consist of five neurons as the optimal structures are used to predict VLE data. Temperature, pressure, and mole fraction of the first compound in the liquid phase ($T$, $P$, $x_1$) were input variables and mole fraction of the first compound in the vapour phase ($y_1$) was output variable. Networks are trained and evaluated by using several sets of collected experimental data. Once the ANN model was trained, estimation of the vapour liquid equilibria data became a straight forward process without any iteration, which it saves computational time considerably. While conventional methods based on EoSs have usually iterative calculation and other complexity, too. In addition developed networks do not require any pure component parameter or the binary interaction parameters, or the mixing rules as required by conventional methods.

Predicted results by using the developed networks were very close to experimental. As deviations was not more than 0.613% for all binary systems. All of these results prove that Artificial Neural Networks can be a successful tool to represent complex nonlinear systems effectively (e.g. prediction of vapour liquid equilibria data), if developed efficiently.

## REFERENCES

[1] H. Yamamoto, K. Tochigi. 2007. Fluid Phase Equilib. 257: 169-172.

[2] V.D. Nguyena, R.R. Tan, Y. Brondial, T. Fuchino. 2007. Fluid Phase Equilib. 254: 188-197.

[3] J.M. Smith, H.C. Van-Ness, M.M. Abbott. 2001. Introduction to Chemical Engineering Thermodynamics, 6th ed., McGraw-Hill, New York.

[4] M.C. Iliuta, O.M. Landauer, F.C. Thyrion. 1998. Fluid Phase Equilib. 149: 163-176.

[5] E. Vercher, M.P. Pena, A.M. Andreu. 1996. J. Chem. Eng. Data. 41: 66-69.

[6] R. Sharma, D. Singhal, R. Ghosh, A. Dwivedi. 1999. Comput. Chem. Eng. 23: 385-390.

[7] S. Ganguly. 2003. Comput. Chem. Eng. 27: 1445-1454.

[8] A. Chouai, S. Laugier, D. Richon. 2002. Fluid Phase Equilib. 199: 53-62.

[9] P. Petersen, A. Fredenslund, P. Rasmussen. 1994. Comput. Chem. Eng. 18: (Suppl. S63-S67).

[10] W.A. Habiballah, R.A. Startzman, M.A. Barrufet. 1994. Proceedings of SPE annual technical conference and exhibition, Reservoir Engineering. 1, 347: (SPE Paper #28597).

[11] P.R.B. Guimaraes, C. McGreavy. 1995. Comput. Chem. Eng. 19: (Suppl.) 741-746.

[12] S. Mohanty. 2006. Int. J. Refrig. 29: 243-249.

[13] H. Ghanadzadeh, H. Ahmadifar. 2008. J. Chem. Thermodyn. 40: 1152-1156.

[14] S. Urata, A. Takada, J. Murata, T. Hiaki, A. Sekiya. 2002. Fluid Phase Equilib. 199: 63-78.

[15] H. Demuth, M. Beale. 2002. Neural Network Toolbox User's Guide, version 4.

[16] J.M. Prausnitz, R.N. Lichtenthaler, E.G. Azevedo. 1999. Molecular thermodynamics of fluid-phase equilibria. 3rd edition, Prentice Hall, New Jersey.

[17] Q.N. Ho, K.S. Yoo, B.G. Lee, J.S. Lim. 2006. Fluid Phase Equilib. 245: 63-70.

[18] S. Bobbo, L. Fedele, R. Camporese, R. Stryjek. 2002. Fluid Phase Equilib. 199: 153-160.

[19] J.H. Kim, M.S. Kim. 2005. Fluid Phase Equilibria. 238: 13-19.

[20] J.H. Kim, M.S. Kim, Y. Kim. 2003. Fluid Phase Equilibria. 211: 273-287.

[21] S. Bobbo, L. Fedele, R. Camporese, R. Stryjek. 2002. Fluid Phase Equilib. 199: 175-183.

[22] M.B. Menhaj. 2002. Introduction of Artificial Neural Network. Amirkabir University Publishing, Iran.

[23] B.G. Lee, W.J. Yang, J.D. Kim, J.S. Lim. 2003. J. Chem. Eng. Data. 48: 841-846.

[24] B.E. Poling, J.M. Prausnitz, J.P. O'Connell. 2001. The Properties of gases and liquids, fifth edition. McGraw-Hill, New York.

[25] J.S. Lim, J.Y. Park, K.S. Lee, J.D. Kim, B.G. Lee. 2004. J. Chem. Eng. Data. 49: 750-755.

[26] G.H. Hanson, R.J. Hogan, W.T. Nelson, M.R. Cines. 1952. Ind. Eng. Chem. 44: 604-608.

[27] A. Harmens. 1985. Chem. Eng. Data J. 30(2): 230-233.

[28] S.E.M. Hamam, B.C.-Y. Lu. 1976. J. Chem. Eng. Data. 21: 200-204.